Co-Registered Solid-State ^{123}i-Mibg Spect And Ct Imaging For The Assessment Of Sympathetic Cardiac Innervation In Healthy Individuals And Variation Over Time

Nikita Nikitin (n_nikitin@outlook.com)
Novosibirskij naucno-issledovatel'skij institut patologii krovoobrasenia imeni akademika E N Meshalkina https://orcid.org/0000-0001-5643-9109

Stanislav Minin
Novosibirskij naucno-issledovatel'skij institut patologii krovoobrasenia imeni akademika E N Meshalkina

James Stirrup
Royal Berkshire Hospital

Evgeny Pokushalov
Novosibirskij naucno-issledovatel'skij institut patologii krovoobrasenia imeni akademika E N Meshalkina

Alexander Romanov
Novosibirskij naucno-issledovatel'skij institut patologii krovoobrasenia imeni akademika E N Meshalkina

Original research

Keywords: Nuclear Medicine, Radionuclide Imaging, Autonomic Nervous System, Ganglionated Plexi, 3-Iodobenzylguanidine, MIBG, SPECT, SPECT/CT, Healthy Volunteers

Posted Date: March 13th, 2020

DOI: https://doi.org/10.21203/rs.3.rs-17077/v1

Abstract

Background. To evaluate global and regional ventricular and atrial cardiac iodine-123 meta-iodobenzylguanidine (123 I-mIBG) uptake and consistency over time in healthy individuals using co-registered SPECT and CT imaging. Fifteen healthy individuals (median age 31 years [26; 41]) were included in the study. All participants underwent CT and subsequent baseline 123 I -mIBG SPECT imaging (early and late acquisition) using a dedicated cardiac solid-state gamma camera. The heart-to-mediastinum (H/M) ratio, wash out rate (WR), summed 123 I-mIBG defect score (SDS) as well as presence and patterns of left atrium (LA) discrete 123 I-mIBG uptake areas were assessed. Follow-up SPECT imaging was acquired 5-7 days after initial procedure.

Results. At baseline median H/M ratio on the early and late acquisitions were 1.61 [1.57; 1.71] and 1.68 [1.65; 1.71] respectively, the WR was 22.5% [18.8; 22.8]. Areas of reduced 123 I-mIBG uptake were detected in 60% (9/15) of cases and the median SDS was 1 [0; 2]. No significant changes were observed in global and regional 123 I-mIBG cardiac uptake between baseline and follow-up studies. At baseline 36 discrete uptake areas (DUA) were identified, 16 (44%) of which (median per individual 1 [1;1]) had moderate-high confidence score (CS). 5/16, 4/16, 4/16 and 3/16 moderate-high CS DUAs were located around the left sided-, right sided- PV ostia, LA walls, right atrium (RA) or superior vena cava (SVC), respectively. At follow-up 33 DUAs were identified, 16 (48%) of which (median per individual 1 [1;1], p=0.5 vs baseline) had moderate-high CS. Moderate-high CS discrete uptake areas had generally the same location as on the baseline procedure.

Conclusion. Co-registered 123 I-mIBG SPECT and CT imaging demonstrated no significant changes in the global and regional 123 I-mIBG cardiac uptake (ventricular and atrial) over a short time interval in healthy individuals.

Background

The autonomic nervous system (ANS) plays an important role in regulating the function of cardiomyocytes, the conducting system, coronary vessels, contractile function of the myocardium, and also affects the electrophysiological properties of the myocardium [1]. The heart is innervated by both the extrinsic (central) and the intrinsic cardiac autonomic nervous system (CANS) [2]. The adrenergic part of CANS can be noninvasively assessed with Iodine-123 metaiodobenzylguanidine (^{123}I-mIBG), which is a sympathetic neurotransmitter radionuclide analog and aids in the detection of sympathetic innervation abnormalities [3]. ^{123}I-mIBG scintigraphy is widely used for the qualitative and quantitative global and regional assessment of cardiac sympathetic innervation and shows cardiac denervation in a variety of pathologies [4].

In recent years, nuclear cardiac imaging has advanced technologically, with the introduction of novel high-sensitivity, rapid-acquisition solid-state dedicated cardiac SPECT cameras. The use of solid-state semiconductor cadmium zinc telluride-based (CZT) detectors, coupled with their ability to fan across the

specific region of interest, has demonstrated significantly improved sensitivity, spatial resolution and energy resolution, enabling cardiac SPECT imaging with a spatial resolution of < 5 mm [5, 6]. Several studies have assessed the comparative performance of Anger-type and CZT SPECT systems for detection of left ventricular myocardial tracers [7–9], but there are few studies evaluating left atrial ^{123}I-mIBG uptake using CZT systems, particularly in healthy individuals. In patients with atrial fibrillation, ^{123}I-mIBG CZT SPECT co-registered with cardiac CT has been reported to identify discrete ^{123}I-mIBG uptake areas (DUAs) non-invasively that correlate with left atrial ganglionated plexi (LAGP) identified invasively by high-frequency stimulation (HFS) during pulmonary vein isolation (PVI) catheter ablation [10]. However, imaging patterns of LAGP in healthy individuals have never been demonstrated. The aim of this study was to evaluate global and regional ventricular and atrial cardiac ^{123}I-mIBG uptake and their consistency over time in healthy individuals using co-registered SPECT and CT imaging.

Methods

Study protocol

The study was initiated in September 2016 to test the feasibility of identifying left atrium ^{123}I-mIBG discrete uptake areas (DUA) in healthy individuals using an imaging technique that enables indirect measurement of cardiac sympathetic innervation, and additionally to evaluate the constancy of CANS imaging patterns.

All study participants underwent an initial assessment including medical history, cardiac CT imaging and ^{123}I-mIBG SPECT imaging. Follow-up ^{123}I-mIBG SPECT imaging was acquired 5–7 days after initial procedure.

Patient Selection

From September 2016 to March 2017 fifteen healthy individuals were consequently included in the study. Inclusion criteria were healthy men or women aged 18–75 years without history or symptoms of heart disease. Exclusion criteria included any history of heart disease, hypertension, diabetes, chronic kidney disease, neuropathy and any contraindication to ^{123}I-mIBG or iodinated contrast media.

Image acquisition and processing

Cardiac computed tomography

All cardiac CT (Aquilion ONE, Toshiba Medical Systems Corp., Japan) scans were performed 1 day prior to ^{123}I-mIBG SPECT imaging. For acquisition of the volume dataset, a biphasic intravenous iodinated contrast protocol was used, with 60 mL contrast at 5 mL/s followed by 30 mL 30%/70% mixture of contrast and normal saline respectively at the same rate. The scan was acquired with prospective ECG triggering in the mid-diastolic phase and in held expiration. Images were imported into dedicated software

(Shina Systems Limited, Caesarea, Israel) for cardiac chamber segmentation. After manual corrections to the segmentation, a representative 3D surface mesh file was created for each chamber, which was then used for co-registration with SPECT images. The mean radiation exposure for the CT procedure was 3.8 +/- 2.1 (3.1–6.5 95% CI) mSv.

^{123} I-mIBG SPECT image acquisition

Imaging procedures were conducted in accordance with established guidelines [11, 15]. All medications known to affect the uptake of ^{123}I-mIBG were ceased and oral thyroid blockade with potassium iodate 170 mg was provided for all patients 1 day before the planned ^{123}I-mIBG administration and continued for 1–2 days afterwards. Medications were re-started following the SPECT procedure. Data were acquired 15 minutes (early acquisition) and four hours (late acquisition) after intravenous injection of 313 +/- 37 (299–327 95% CI) MBq ^{123}I-mIBG, on a dedicated cardiac solid-state SPECT camera (D-SPECT, Spectrum Dynamics Medical, Caesarea, Israel) with cardiac- and respiratory-gating. Study acquisition time was 20 minutes. The mean radiation exposure for the SPECT procedure was 4.11 +/- 0.5 (3.9–4.3 95% CI) mSv [12].

^{123} I-mIBG SPECT and CT image processing and co-registration

To process the corresponding SPECT and CT images, ^{123}I-mIBG late acquisition datasets were reconstructed with a high-resolution reconstruction algorithm in the diastolic phase of the cardiac cycle and in the expiratory phase of the respiratory cycle.

The co-registered images were generated using a dedicated workstation (SUMO D-SPECT, Spectrum Dynamics Medical, Caesarea, Israel). SPECT images were automatically co-registered to the CT images using left ventricular (LV) myocardial uptake as the SPECT reference and LV myocardial segmentation as the CT reference. The SPECT tomograms could be translated in the (x, y, z) direction in order to achieve accurate location matching with the CT-derived myocardial segmentation using identifiable anatomic reference points (ie. left ventricular apex and mitral annulus). Co-registration accuracy was reviewed by scrolling through horizontal long, vertical long and short axis views and, once satisfactory alignment was confirmed, final 3D images of cardiac innervation combined with anatomical information were generated.

Data analysis

Global and regional sympathetic cardiac innervation

The planar equivalent image (planogram) was used to derive heart-to-mediastinum (H/M) ratio for the early and late acquisitions, which in turn were used to calculate cardiac wash out rate (WR) [13]. The H/M ratio was determined from the average pixel counts/number of pixels in a visually drawn heart region of interest (ROI) divided by the average pixel counts/number of pixels in a visually drawn mediastinum ROI in the midline upper chest positioned to reflect the region with lowest background activity. The WR was calculated as described elsewhere [15].

For SPECT image analysis, regional myocardial ^{123}I-mIBG uptake was classified using a 17-segment model of the left ventricle and a semiquantitative five-point scale (0 = normal uptake, 1 = mildly reduced uptake, 2 = moderately reduced uptake, 3 = severely reduced uptake and 4 = no uptake). Readers were instructed that scoring could be adjusted if artefact was thought to be present. A summed ^{123}I-mIBG defect score (SDS) was calculated as the sum of all segmental defect scores in the late acquisition; patients with no defect were scored zero. Scoring was performed independently by two experienced nuclear physicians and consensus was reached in case of divergence.

Co-registered ^{123}I-mIBG SPECT/CT data analysis

Focal areas of increased ^{123}I-mIBG activity around the left atrium were reviewed and accepted or rejected by the reader as discrete uptake areas (DUAs). Each DUA was assigned a confidence score (CS) based on discreteness, extent of overlap with non-LA activity (e.g. LV myocardium or lung) and proximity to known anatomical GP cluster locations. DUAs that met all three criteria – discrete, distinct from adjacent extracardiac activity and located in an area known to be typical for GPs – were scored with high CS. DUAs meeting only 2 or 1 of the criteria were scored with moderate and low CS respectively. Areas of uptake adjacent to areas of known high 123I-mIBG activity, such as the basal lateral wall of the LV, lung or anterior to the esophagus were scored with lower confidence or excluded from consideration. Images were reviewed for the identification of DUA and a final CS assigned by a consensus of blinded analyses by 3 trained physicians (1 radiologist and 2 electro- physiologists).

Statistics

Descriptive statistics are presented as median [interquartile range] for continuous variables and are frequencies and percentages of patients for categorical variables. Differences in median values, where appropriate, were analyzed using either the Wilcoxon signed rank test for paired samples or the Mann–Whitney U test for unpaired samples. All the presented p-values were based on a two-sided test and a p-value < 0.05 was considered statistically significant.

Results

All 15 healthy participants in the study completed both baseline and follow-up imaging protocols. The clinical and demographic data are detailed in Table 1.

Table 1

Clinical and demographic characteristics of study participants. Me – median; IQR – interquartile range.

Characteristic	Me / Value (%)	Range [IQR]
Age, years	31	[26; 41]
Females, n	7 (47%)	
BMI, (kg/m^2)	24	[22; 26]
Smokers, n	4 (27%)	
Hypertension, n	0 (0%)	
Diabetes mellitus, n	0 (0%)	
Cardiovascular disease, n	0 (0%)	

Table 2

^{123}I-mIBG global and regional cardiac uptake analysis. Me – median; IQR – interquartile range. H/M – heart-to-mediastinum; WR –washout rate; SDS – summed defect score.

Variable	Baseline, Me [IQR]	Follow-up, Me [IQR]	p
Early H/M ratio	1.61 [1.57; 1.71]	1.7 [1.62; 1.74]	0.51
Late H/M ratio	1.68 [1.65; 1.71]	1.69 [1.66; 1.75]	0.94
WR, %	22.5 [18.8; 22.8]	21.9 [19.5; 26.2]	0.96
SDS	0 [1; 2]	1 [0; 1]	0.1

Table 3

Co-registered ^{123}I-mIBG SPECT/CT data analysis. n – numbers; Me – median; IQR – interquartile range; DUA – discrete mIBG uptake area; CS – confidence level;

Variable		Baseline (n = 15)	Follow-up (n = 15)	p
Total number of DUAs, n		36	33	0.9
Average amount of DUA per individual, Me [IQR]		2 [2;3]	2 [2;2.5]	0.42
Moderate to high CS DUA	Total number, n (%)	16 (44%)	16 (48%)	0.99
	Average number, Me [IQR]	1 [1;1]	1 [1;1]	0.5

Global and regional sympathetic cardiac innervation

No significant changes were observed in global and regional ^{123}I-mIBG cardiac uptake between baseline and follow-up studies. Median [interquartile range] early H/M ratio was 1.61 [1.57; 1.71] at baseline and 1.7 [1.62; 1.74] at follow-up (p = 0.51). Median late H/M ratio was 1.68 [1.65; 1.71] at baseline and 1.69 [1.66; 1.75] at follow-up (p = 0.94). The WR were 22.5% [18.8; 22.8] at baseline and 21.9% [19.5; 26.2] at follow-up (p = 0.96).

^{123}I-mIBG reduced uptake areas were detected in 60% (9/15) of the healthy volunteers at baseline and in 53% (8/15) at follow-up studies. These areas were located mostly at the LV apex (7/15 participants at baseline and 6/15 at follow-up), and in the apical or basal segments of LV inferior wall (5/15 participants at baseline and 3/15 at follow-up). The median SDS was 1 [0; 2] at baseline and 1 [0; 1] at follow-up (p = 0.1).

Co-registered ^{123}I-mIBG SPECT/CT data

At baseline 36 DUAs were identified around the left atrium, of which 20 (56%) had low CS and 16 (44%) (median per individual 1 [1;1]) had moderate-high CS. Moderate-high CS DUAs were located with more or less frequency in the area around left superior pulmonary vein (corresponding to anatomical cluster of left superior GP, Fig. 1) as around the ostium of right superior PV (corresponding to anatomical cluster of right anterior GP) – 5/16 and 4/16 DUAs respectively. 3/16 DUAs were located at the junction of superior vena cava (SVC) and right atrial (RA) surface of the interatrial septum (Fig. 2).

At follow-up 33 DUAs were identified, 16 (48%) of which (median per individual 1 [1;1], p = 0.5 vs baseline) had moderate-high CS. Moderate-high CS DUAs had rather widest anatomical distribution – 2/16 DUAs were located in interatrial septum, left superior, right anterior clusters; 5/15 DUAs were located at the junction of SVC and RA (Fig. 3).

10/16 (63%) DUAs identified at baseline with moderate-high CS were seen in the same location at follow-up. This was only true for 2/20 (10%) DUAs identified with low confidence at baseline. 6/16 (37%) moderate-high CS DUAs identified at baseline were not reproduced on the follow-up study.

Discussion

In this study, we demonstrated for the first time the feasibility for identification of left atrium ^{123}I-mIBG discrete uptake areas (DUA) in healthy individuals using co-registered images from ^{123}I-mIBG solid-state SPECT and a corresponding CT. Also, we evaluated imaging patterns of atrial and ventricular cardiac sympathetic innervation and their variation over time in a small cohort of healthy individuals.

Originally developed as a radionuclide for imaging adrenal tumors, ^{123}I-mIBG has emerged as a promising tool for the prediction of heart failure progression [16], arrhythmic events [17], and even prognosis of AF recurrence after interventional treatment [18]. More recently, imaging with dedicated

cardiac SPECT cameras using solid-state CZT detectors has been shown to identify discrete areas of sympathetic activity that correlate with GPs identified invasively using high frequency stimulation (HFS) [10].

Global and regional sympathetic cardiac innervation

Late H/M ratio determination using the planar images from Anger SPECT cameras (A-SPECT) is a well-standardized and reproducible parameter in assessment of global sympathetic cardiac innervation and its prognostic value is widely recognized. However, previous studies using A-SPECT cameras have shown that the acquisition protocol used significantly affects quantification of late ^{123}I-mIBG H/M ratio. In particular the collimators used and the stopping power of the detector material may have an impact on the quantification of the ^{123}I-mIBG H/M ratio [19].

Also, it has been noted that there are a growing number of nuclear medicine sites that are using the new generation of cardiac-centered CZT-based gamma cameras for routine clinical practice [20]. That suggests the importance of developing further clinical evidence regarding the assessment of ^{123}I-mIBG cardiac uptake features using such dedicated cardiac SPECT cameras. It has been demonstrated that these cameras have a better count detection sensitivity and improved energy resolution, enabling reductions in acquisition times and injected radiopharmaceutical doses [5, 6]. However, there are only a small number of studies evaluating cardiac sympathetic innervation imaging with these new generation detectors [21–23] and only a few studies have compared H/M ratio determined using CZT acquisition versus that determined using A-SPECT [13, 14]. Bellevre et al. demonstrated that determination of the late H/M ratio of ^{123}I-MIBG uptake using a parallel-collimator CZT camera (D-SPECT, Spectrum Dynamics Medical, Caesarea, Israel) was feasible, reliable and equivalent to H/M ratio using A-SPECT in patients with heart failure [13]. It has also been noted that H/M ratio values from D-SPECT were significantly higher than those from A-SPECT, however after applying a correction factor, there was no significant difference between A-SPECT H/M ratio and corrected D-SPECT H/M ratio. In contrast, Blaire et al. using a multi-pinhole CZT camera (Discovery NM 530c, GE Healthcare) found almost perfect concordance between H/M ratio derived from transaxial SPECT images and H/M ratio from planar ones however concordance between H/M ratio from re-projected images and planar ones was only moderate. Blaire et al. considered that was related to the multi-pinhole collimation, which is responsible for a truncation artifact that interferes with the mean counts of the myocardial ROI [14].

In our study we used the methodology of H/M ratio calculation proposed Bellevre et al. [13]. Thus, quantitative characteristics of global sympathetic activity (H/M ratio, WR) from our study are comparable to those in a recent study of healthy adults [24] that used planar images for calculation and are lower than reported in ADMIRE-HF study controls participants that used SPECT-derived data [25]. This fact may sustain the methodology of H/M ratio determination using planogram images and a correction factor as the data source for the cardiac dedicated parallel-collimator CZT camera (D-SPECT, Spectrum Dynamics Medical, Caesarea, Israel) used in this study.

A recent study of healthy adults (n = 15) with mean age 54.6 ± 5.4 reported heterogeneous patterns of regional ^{123}I-mIBG uptake predominantly affecting the LV apex, base and inferior wall [24]. This is in concordance with earlier observational studies that reported the effects of age and sex on myocardial ^{123}-mIBG uptake [26, 27]. The recent ADMIRE-HF study, however, failed to show an influence of age on ^{123}I-mIBG uptake in older healthy controls [25]. In our study, we also observed a slight decreasing of ^{123}I-mIBG regional myocardial uptake comprised mostly of mild uptake reduction in LV apex and LV inferior wall segments. The low median age of our participants (31 years [26;41]) makes, however, the abovementioned age-related denervation an unlikely contributor to our findings. Our study subjects also did not have hypertension, diabetes mellitus or any other disease known to affect the autonomic nervous system. Decreased regional myocardial ^{123}I-mIBG uptake has previously been reported in athletes, in the setting of both normal heart rate and sinus bradycardia [28]. In this cohort, inferior, apical and septal defects were all demonstrated, with a significant reduction in percentage regional ^{123}I-mIBG uptake in the inferior region for athletes with sinus bradycardia. Additionally, a normal SPECT database accumulated by the Japanese Society of Nuclear Medicine (JSNM) working group evaluating normal values and standardization of parameters in nuclear cardiology found patterns of lower count distribution of ^{123}I-mIBG, particularly in the inferior region [33], as we have shown in the cohort of healthy individuals studied here. Hence, the slight decreases in ^{123}I-mIBG regional myocardial uptake in our study subjects can be interpreted as a heterogeneous pattern of regional myocardial ^{123}I-mIBG uptake and indicate normal physiological variation.

Co-registered ^{123}I-mIBG SPECT/CT data

According to the results of a recent study, pre-operative non-invasive imaging of ^{123}I-mIBG DUAs may be helpful in targeting locations for LAGP ablation as a part of interventional AF treatment. This may potentially increase the efficacy of the ablation procedure without touching viable myocardium during LAGP detection using HFS [29]. Hence, knowledge of the distribution and characteristics of DUAs in humans without cardiovascular disease may be helpful for future studies of image-guided AF ablation procedures.

Our study of healthy individuals demonstrates the presence of discrete uptake of ^{123}I-mIBG, a radiolabeled analog of sympathetic neuronal transmitter norepinephrine, around the left atrium. This fact allows us to assume the presence of sympathetic activity areas in sites that correspond to known anatomical clusters of LAGP. The Oklahoma research group have localized and named the major sites around the left atrium that contain autonomic neurons based on response to HFS, thereby facilitating improved communication among clinical electrophysiologists. These are the anterior right GP, the superior left GP, the right and left inferior GP and the ligament of Marshal [30]. Several studies have shown that LAGPs contain both sympathetic and parasympathetic elements, as well as a variety of neuropeptides and neuromodulators [31, 32]. Hence, physiological ^{123}I-mIBG uptake in typical anatomical sites serves as a marker for LAGP location. For ethical reasons, we did not proceed to confirm the DUAs

identified in our normal patient cohort invasively with HFS, but this has been done in patients with paroxysmal AF [10].

In comparison with a recent study of AF patients (n = 21) [10] we found a much smaller number of DUAs in healthy individuals (4 [3-4.5] vs 1 [1;1]). However, it should be noted that discrete ^{123}I-mIBG uptake could indicate only the presence of local sympathetic neurotransmission functional activity, but not the presence of anatomical (or material) structures. The relationship between left atrial sympathetic activity and atrial fibrillation requires further investigation but our data could suggest that healthy individuals seem to have fewer functionally active GPs than has been reported for patients with AF.

In our study, we demonstrate that DUAs corresponding to the described anatomical LAGP sites are more frequently reproduced in follow-up studies (10/16 (63%)) than DUAs located in other LA areas, corroborating the idea that these sites reflect true LAGPs. It seems that in general, the only slight variations in reproducibility of DUAs imaging, hypothetically could be related with functional changes in CANS activity.

Limitations Of The Study

The primary limitation of the present study is the small number of subjects included. In addition, we did not apply any cardiac testing to confirm the healthy status of study participants. Also, the variability in the positions of the ^{123}I-mIBG discrete uptake areas between the baseline and follow-up studies may, at least in part, be camera related or due to subject positioning or even the appearance of true new uptake areas. A larger study is required to confirm our findings. Also, there is need for further research to correlate imaging findings with morphological studies of presumed LAGP locations.

New Knowledge Gained

Global and regional 123I-mIBG cardiac uptake, taken as an indirect marker of cardiac autonomic nervous system functional activity, remained constant over a short time interval in healthy individuals. Discrete uptake areas of 123I-mIBG in the typical anatomical sites of left atrial ganglionated plexi could be visualized in healthy individuals with only slight variations in the constancy of uptake locations. Thus, the further investigation on imaging patterns and their diagnostic significance is needed.

Conclusion

Co-registered ^{123}I-mIBG SPECT/CT imaging is feasible to visualize left atrium discrete ^{123}I-mIBG uptake areas in healthy individuals. No significant changes in the global and regional ^{123}I-mIBG cardiac uptake (ventricular and atrial) were observed over a short time interval in healthy individuals.

Abbreviations

DUA
discrete uptake area
^{123}I-mIBG
Iodine-123 metaiodobenzylguanidine
CZT
cadmium-zinc-telluride
CT
computed tomography
SPECT
single-photon emission computed tomography
H/M
heart-to-mediastinum
WR
wash out rate
SDS
summed ^{123}I-mIBG defect score
CS
confidence score
LA
left atrium
LV
left ventricle
LAGP
left atrial ganglionated plexi
ICRP
International Commission on Radiological Protection
HFS
high-frequency stimulation

Declarations

Ethics approval and consent to participate. The study protocol was approved by the Local Medical Ethics Committee of Meshalkin National Medical Research Center. Written informed consent, according to the declaration of Helsinki, was obtained from all participants.

Consent for publication. Consent for publication of results was obtained through the informed consent form which was signed by each subject before any trial-related procedures were performed.

Availability of data and material. The datasets generated during the current study are available from the corresponding author on reasonable request.

Competing interests. The authors declare that they have no competing interests.

Funding. This study was supported by grants from the Russian Science Foundation (project No. 17-75-20118).

Authors' contributions. The study design was set up by SM, EP and AR. Data collection and interpretation was carried out by NN, SM and JS. AR was the principal investigator of this study. All authors read and approved the final manuscript.

Acknowledgements. The authors wish to thank Magnus Holm and Justine McQuillan (employees of Spectrum Dynamics Medical, Caesarea, Israel) for language revision of the manuscript.

Authors' information. Nikita Nikitin's presentation of a part of this study was recognized as the best original scientific work at Talent of the future section which held on 14th International Conference on Nuclear Cardiology and Cardiac Computed Tomography. A thesis of this study was referenced in «Highlights of the 14th International Conference on Nuclear Cardiology and Cardiac Computed Tomography», Hayfil et al. (2020), Eur Heart J Cardiovasc Imaging at http://doi.org/10.1093/ehjci/jez223

References

1. Battipaglia I, Lanza GA. Chapter 1: The Autonomic Nervous System of the Heart. In: Autonomic Innervation of the Heart. New York City: Springer Publishing; 2015. p. 1-12.
2. Stavrakis S, Po S. Ganglionated Plexi Ablation: Physiology and Clinical Applications. Arrhythm Electrophysiol Rev. 2017;6(4):186–190. doi:10.15420/aer2017.26.1
3. Chirumamilla A, Travin MI. Cardiac applications of 123I-mIBG imaging. Semin Nucl Med. 2011 Sep;41(5):374-87. doi:10.1053/j.semnuclmed.2011.04.001. Review.
4. Carrió I, Flotats A. Expanding indications for cardiac mIBG imaging of sympathetic activity. Eur J Nucl Med Mol Imaging 2011 Feb;38(2):219-20. doi:10.1007/s00259-010-1650-7.
5. Gambhir SS, Berman DS, Ziffer J, Nagler M, Sandler M, Patton J, et al. A Novel High-Sensitivity Rapid-Acquisition Single-Photon Cardiac Imaging Camera. J Nucl Med. 2009 Apr 1;50(4):635– 43. doi:10.2967/jnumed.108.060020
6. Imbert, L. & Marie, PY. CZT cameras: A technological jump for myocardial perfusion SPECT. J. Nucl. Cardiol. (2016) 23: 894. doi:10.1007/s12350-015-0216-2
7. Songy B, Lussato D, Guernou M, Queneau M, Geronazzo R. Comparison of myocardial perfusion imaging using thallium-201 between a new cadmium-zinc-telluride cardiac camera and a conventional SPECT camera Clin Nucl Med. 2011 Sep;36(9):776-80. doi:10.1097/RLU.0b013e31821a294e
8. Nudi F, Biondi-Zoccai G. Cadmium-zinc-telluride myocardial perfusion imaging: The dream of a single test gets nearer. J Nucl Cardiol. 2018 Apr;25(2):550-554. doi:10.1007/s12350-017-0833-z

9. Gimelli A, Liga R, Menichetti F, Soldati E, Bongiorni MG, Marzullo P. Interactions between myocardial sympathetic denervation and left ventricular mechanical dyssynchrony: A CZT analysis. J Nucl Cardiol. 2019;26(2):509–518. doi:10.1007/s12350-017-1036-3
10. Stirrup J, Gregg S, Baavour R, Roth N, Breault C, Agostini D, et al. Hybrid solid-state SPECT/CT left atrial innervation imaging for identification of left atrial ganglionated plexi: Technique and validation in patients with atrial fibrillation. J Nucl Cardiol. 2019 Jan 29. doi:10.1007/s12350-018-01535-5
11. Bombardieri E, Giammarile F, Aktolun C, et al. 131I/123I-metaiodobenzylguanidine (mIBG) scintigraphy: procedure guidelines for tumour imaging. Eur J Nucl Med Mol Imaging. 2010;37(12):2436–2446. doi10.1007/s00259-010-1545-7
12. ICRP, 1998. Radiation Dose to Patients from Radiopharmaceuticals (Addendum to ICRP Publication 53). ICRP Publication 80. Ann. ICRP 28 (3).
13. Bellevre D, Manrique A, Legallois D, Bross S, Baavour R, Roth N et al. First determination of the heart-to-mediastinum ratio using cardiac dual isotope (^{123}I-mIBG/^{99m}Tc-tetrofosmin) CZT imaging in patients with heart failure: the ADRECARD study. Eur J Nucl Med Mol Imaging. 2015 Nov;42(12):1912-9. doi:10.1007/s00259-015-3141-3
14. Blaire T, Bailliez A, Ben Bouallegue F, Bellevre D, Agostini D, Manrique A. Determination of the Heart-to-Mediastinum Ratio of 123I-MIBG Uptake Using Dual-Isotope (123I-MIBG/99mTc-Tetrofosmin) Multipinhole Cadmium-Zinc-Telluride SPECT in Patients with Heart Failure. J Nucl Med. 2018;59(2):251–258. doi:10.2967/jnumed.117.194373
15. Flotats A, Carrio I, Agostini D, Le Guludec D, Marcassa C, Schafers M, et al. Proposal for standardization of 123I-metaiodobenzylguanidine (mIBG) cardiac sympathetic imaging by the EANM Cardiovascular Committee and the European Council of Nuclear Cardiology. Eur J Nucl Med Mol Imaging 2010, 37:1802–1812. doi:10.1007/s00259-010-1491-4
16. Verschure DO, Veltman CE, Manrique A, Somsen GA, Koutelou M, Katskis A et al. For what endpoint does myocardial 123I-mIBG scintigraphy have the greatest prognostic value in patients with chronic heart failure? Results of a pooled individual patient data meta-analysis. Eur Heart J Cardiovasc Imaging. 2014 Sep;15(9):996–1003. doi:10.1093/ehjci/jeu044
17. Marshall A, Cheetham A, George RS, Mason M, Kelion AD. Cardiac iodine-123 metaiodobenzylguanidine imaging predicts ventricular arrhythmia in heart failure patients receiving an implantable cardioverter-defibrillator for primary prevention. Heart 2012;98:1359-65. doi:10.1136/heartjnl-2012-302321
18. Arimoto T, Tada H, Igarashi M, Sekiguchi Y, Sato A, Koyama T, et al. High washout rate of iodine-123-metaiodobenzylguanidine imaging predicts the outcome of catheter ablation of atrial fibrillation. J Cardiovasc Electrophysiol. 2011 Dec;22(12):1297–304. doi:10.1111/j.1540-8167.2011.02123.x
19. Verberne HJ, Feenstra C, de Jong WM, Somsen GA, van Eck-Smit BL, Busemann Sokole E. Influence of collimator choice and simulated clinical conditions on 123I-MIBG heart/mediastinum ratios: a phantom study. Eur J Nucl Med Mol Imaging. 2005;32:1100–1107. doi:10.1007/s00259-005-1810-3

20. Hyafil, F., Gimelli, A., Slart, R.H.J.A. et al. EANM procedural guidelines for myocardial perfusion scintigraphy using cardiac-centered gamma cameras. European J Hybrid Imaging 3, 11 (2019) doi:10.1186/s41824-019-0058-2
21. Gimelli A, Liga R, Genovesi D, Giorgetti A, Kusch A, Marzullo P. Association between left ventricular regional sympathetic denerva- tion and mechanical dyssynchrony in phase analysis: a cardiac CZT study. Eur J Nucl Med Mol Imaging. 2014;41:946–55. doi:10.1007/s00259-013-2640-3
22. Gimelli A, Liga R, Giorgetti A, Genovesi D, Marzullo P. Assessment of myocardial adrenergic innervation with a solid- state dedicated cardiac cadmium-zinc-telluride camera: first clinical experience. Eur Heart J Cardiovasc Imaging. 2014;15:575–85. doi:10.1093/ehjci/jet258
23. Tinti E, Positano V, Giorgetti A, Marzullo P. Feasibility of [(123)I]- meta-iodobenzylguanidine dynamic 3-D kinetic analysis in vivo using a CZT ultrafast camera: preliminary results. Eur J Nucl Med Mol Imaging. 2014;41:167–73. doi:10.1007/s00259-013-2549-x
24. Asghar O, Arumugam P, Armstrong I, Ray S, Schmitt M, Malik RA. Iodine-123 metaiodobenzylguanidine scintigraphy for the assessment of cardiac sympathetic innervation and the relationship with cardiac autonomic function in healthy adults using standardized methods. Nucl Med Commun. 2017 Jan;38(1):44-50. doi:10.1097/MNM.0000000000000608
25. Chen, J, Folks, RD, Verdes, L. et al. Quantitative I-123 mIBG SPECT in differentiating abnormal and normal mIBG myocardial uptake. J. Nucl. Cardiol. (2012) 19: 92-99. doi:10.1007/s12350-011-9438-0
26. Gill JS, Hunter GJ, Gane G, Camm AJ. Heterogeneity of the human myocardial sympathetic innervation: in vivo demonstration by iodine 123-labeled meta-iodobenzylguanidine scintigraphy. Am Heart J 1993; 126:390–398. doi:10.1016/0002-8703(93)91056-k
27. Sakata K, Shirotani M, Yoshida H, Kurata C. Physiological fluctuation of the human left ventricle sympathetic nervous system assessed by iodine-123-mIBG. J Nucl Med. 1998 Oct;39(10):1667-71.
28. Estorch M, Serra-Grima R, Flotats C, Marí C, Bernà L, Catafau A, Martín JC, Tembl A, Narula J, Carrió I. Myocardial sympathetic innervation in the athlete's bradycardia: is there selective inferior myocardial wall denervation? J Nucl Cardiol. 2000 Jul-Aug;7(4):354-8. doi:10.1067/mnc.2000.105550
29. Romanov A, Minin S, Breault C, Pokushalov E. Visualization and ablation of the autonomic nervous system corresponding to ganglionated plexi guided by D-SPECT 123I-mIBG imaging in patient with paroxysmal atrial fibrillation. Clin Res Cardiol. 2017 Jan;106(1):76-78. doi:10.1007/s00392-016-1045-2.
30. Po SS, Nakagawa H, Jackman WM. Localization of left atrial ganglionated plexi in patients with atrial fibrillation. J Cardiovasc Electrophysiol 2009;20:1186–9. doi:10.1111/j.1540-8167.2009.01515.x
31. Hoover DB, Isaacs ER, Jacques F, et al. Localization of multiple neurotransmitters in surgically derived specimens of human atrial ganglia. Neuroscience 2009;164:1170–9. doi:10.1016/j.neuroscience.2009.09.001
32. Steele PA, Gibbins IL, Morris JL, Mayer B. Multiple populations of neuropeptide-containing intrinsic neurons in the guinea- pig heart. Neuroscience 1994;62:241–50. doi:10.1016/0306- 4522(94)90327-

1

33. Nakajima K, Matsumoto N, Kasai T, Matsuo S, Kiso K, Okuda K. Normal values and standardization of parameters in nuclear cardiology: Japanese Society of Nuclear Medicine working group database. Ann Nucl Med. 2016 Apr;30(3):188-99. doi:10.1007/s12149-016-1065-z

Figures

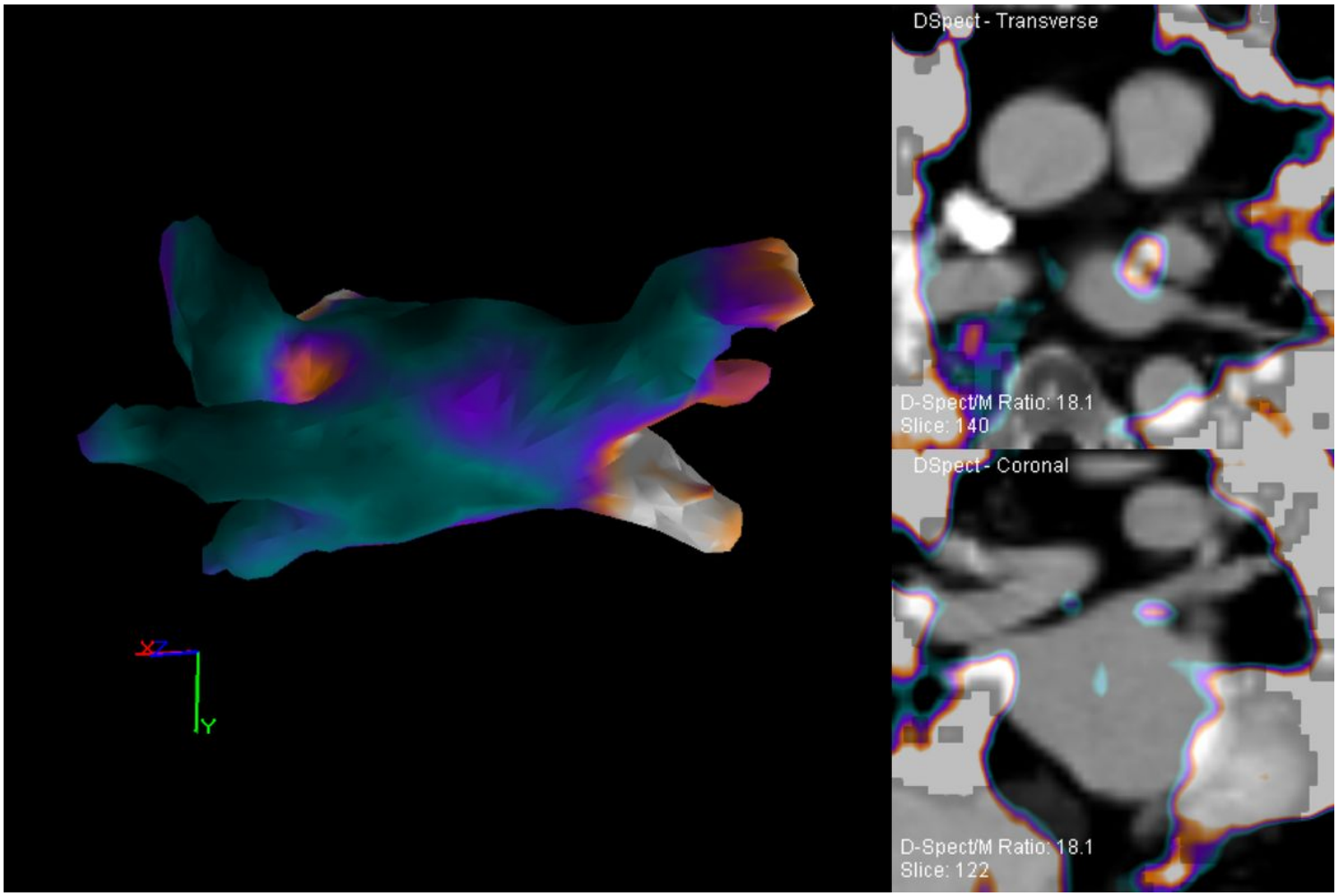

Figure 1

(a) PA view of co-registered 123I-mIBG SPECT/CT LA surface. DUA on the LA surface (asterix), compatible with a typical location of the left superior ganglionated plexus. Axial (b) and coronal (c) co-registered SPECT/CT images of the same case.

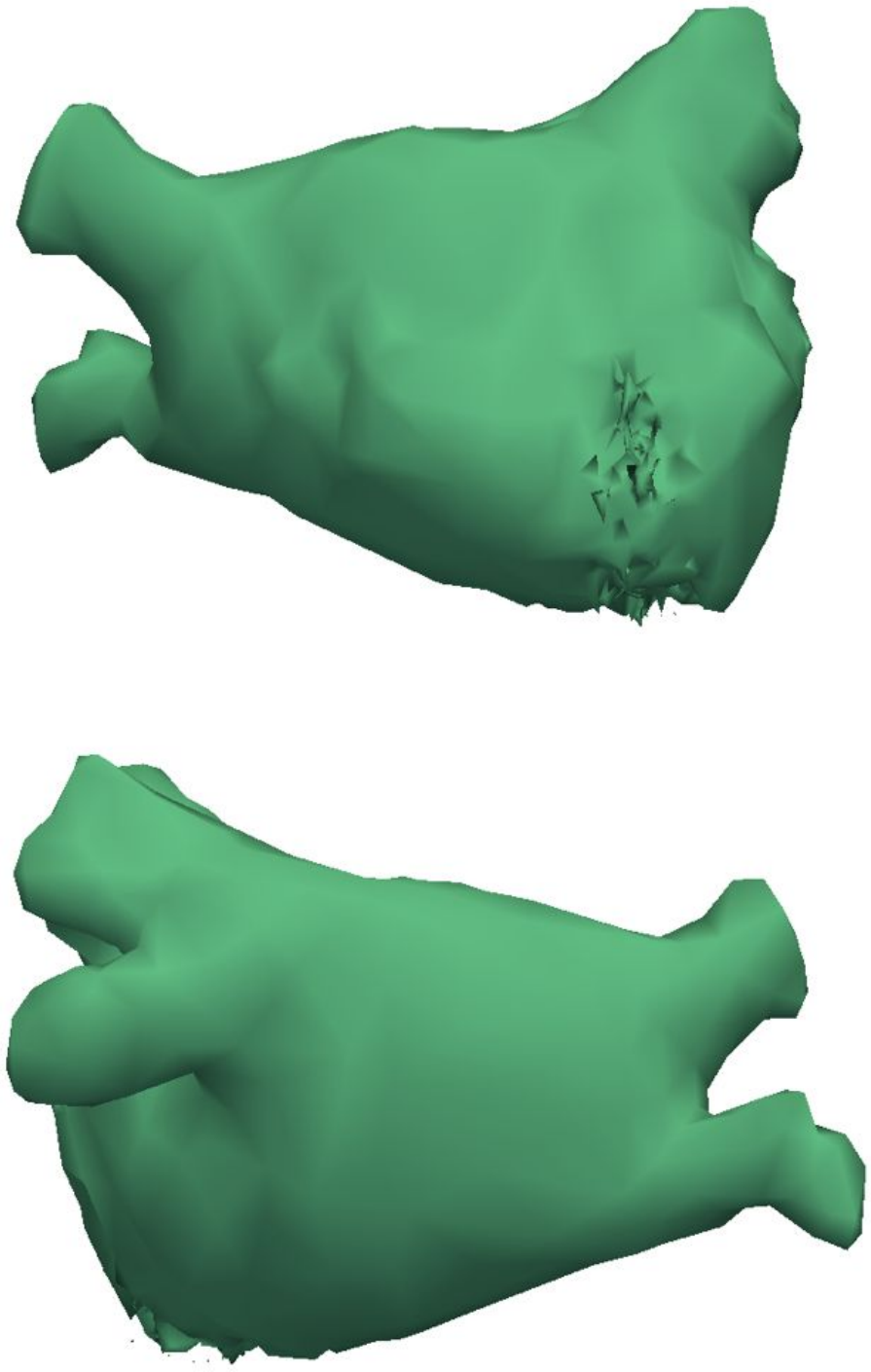

Figure 2

AP (a) and PA (b) views of CT-derived LA surfaces demonstrate the frequency of DUAs distribution in baseline studies.

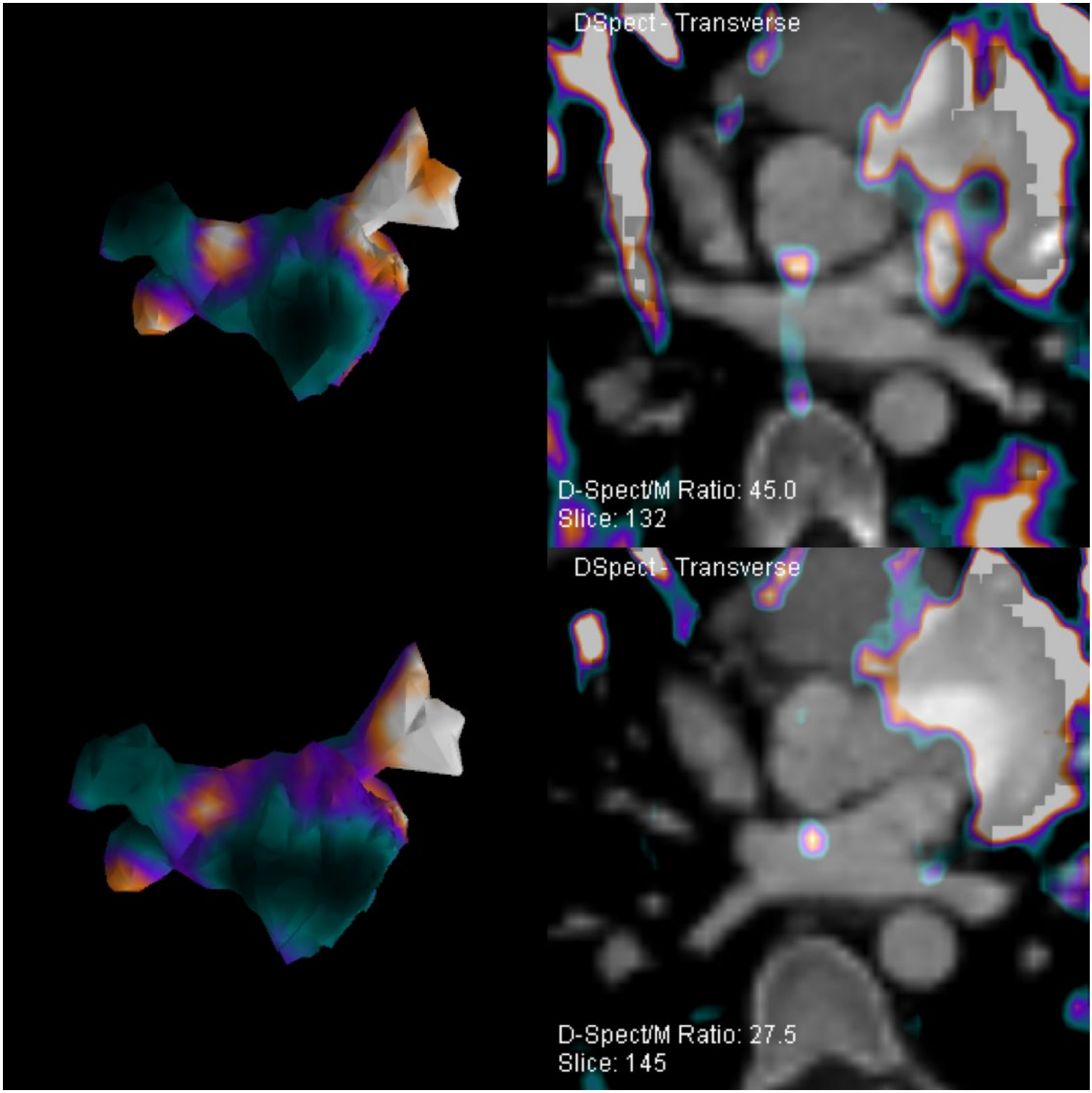

Figure 3

(a, c) baseline study and (b, d) follow-up study of the same participant. (a, b) AP views of co-registered 123I-mIBG SPECT/CT LA surface. DUA on the LA surface (asterix), compatible with a typical location of the right anterior ganglionated plexus. (b, d) axial co-registered SPECT/CT images.